ISSN 0030-400X, Optics and Spectroscopy, 2017, Vol. 123, No. 5, pp. 728–732. © Pleiades Publishing, Ltd., 2017.
Original Russian Text © V.A. Shvets, V.N. Kruchinin, V.A. Gritsenko, 2017, published in Optika i Spektroskopiya, 2017, Vol. 123, No. 5, pp. 728–733.

CONDENSED-MATTER SPECTROSCOPY

Dispersion of the Refractive Index in High-*k* Dielectrics

V. A. Shvets[a, b, *], V. N. Kruchinin[a], and V. A. Gritsenko[a, b, c]

[a] *Rzhanov Institute of Semiconductor Physics, Siberian Branch, Russian Academy of Sciences, Novosibirsk, 630090 Russia*

[b] *Novosibirsk State University, Novosibirsk, 630090 Russia*

[c] *Novosibirsk State Technical University, Novosibirsk, 630073 Russia*

**e-mail: shvets@isp.nsc.ru*

Received May 31, 2017

Abstract—A brief review of the optical properties of oxide materials that are used at present as dielectrics in modern microelectronics is presented. Using spectral ellipsometry, dispersion dependencies for different materials are measured. A brief comparative analysis of different dielectric coatings is carried out. The results of our research will be useful in further studies of the properties of dielectrics, as well as in technologies that are employed in the development of new semiconductor instruments and devices.

DOI: 10.1134/S0030400X17110194

INTRODUCTION

Dielectric films have been widely used in optical devices, such as interference filters, antireflection coatings, semiconductor solar energy converters, and multilayer laser mirrors with selective properties, as well as in the capacity of protective coatings in nonlinear frequency converters of laser radiation.

In semiconductor instruments, dielectric films are used as gate dielectrics, in field-effect transistors, as insulating and passivating layers, and, in flash memory devices, as a memory medium [1]. Over the past five decades, silicon dioxide, SiO_2, the high-frequency permittivity of which is $k = 3.9$, has been used as a gate dielectric in silicon devices. At present, dielectrics with a high value of the dielectric permittivity (the so-called high-k dielectrics) appear to replace silicon dioxide. Compounds of this kind include Al_2O_3 ($k = 9$), HfO_2 ($k = 25$), ZrO_2 ($k = 25$), Ta_2O_5 ($k = 25$), TiO_2 ($k = 80$), and oxides of rare-earth elements, such as La_2O_3, Y_2O_3, Lu_2O_3, Sc_2O_3, Dy_2O_3, Gd_2O_3, Ho_2O_3, Yb_2O_3, and Er_2O_3 ($k = 12–16$) [2, 3]. The latter compounds have large band-gap widths, $E_g \approx 5–6$ eV, and, as a consequence, high barriers for injection of electrons and holes and high breakdown-field strengths.

At present, a new generation of high-speed, radiation-resistant, and nonvolatile resistive flash memory of a terabit scale is developing using these dielectrics. The resistive memory is based on a memristor, a resistance the magnitude of which depends on the amount of charge that flows through it. At present, SiO_2 [4], GeO_2 [5], Si_3N_4 [6], HfO_2 [7], ZrO_2 [8], Ta_2O_5 [9], and oxides of rare-earth elements [10] are intensely studied as an active medium of memristors. A promising trend in the development of a terabit memory device is the recently discovered effect of ferroelectric memory in $Hf_{0.5}Zr_{0.5}O_2$ films [11].

Refractive index n is an important parameter of dielectric films. It specifies the value of the reflection coefficient. The value of the high-frequency permittivity ε_∞ in the transparency range of a dielectric is equal to the squared refractive index, $\varepsilon_\infty = n^2$. Except for thermal silicon oxide, all dielectric films have a high concentration of traps. The localization of electrons and holes and the conductivity of these films are limited by the ionization of traps in a strong electric field. In turn, the ionization of traps is limited by the multiphonon mechanism or the Frenkel effect [12]. The Frenkel effect consists of lowering the Coulomb potential in an electric field [13], which depends on the magnitude of the high-frequency dielectric permittivity, i.e., on the value of the refractive index [14]. The functional properties of optical elements and devices depend on the value of the refractive index of used layers. To apply optical methods for controlling technological processes when growing dielectric layers, reliable databases on optical constants are also required.

An important problem is to study the mechanism of charge transport in the active medium of a memristor and a ferroelectric memory element. One possible mechanism for the ionization of traps is the Frenkel effect, the importance of the knowledge of the refractive index for which was discussed above.

Table 1. Results of calculations of the coefficients of the Cauchy dispersion model for oxide films of high-*k* dielectrics

Material	Spectral range, nm	Parameters of the Cauchy model			*n* (632.8 nm)	Synthesis method
		n_0	A, $\times 10^{-4}$	B, $\times 10^{-9}$		
Oxides of rare-earth metals						
Sc_2O_3	250–800	1.956	–0.118	1.440	1.962	TE
Y_2O_3	250–800	1.692	1.932	0.105	1.741	TE
La_2O_3	250–800	1.722	1.268	0.090	1.754	TE
Gd_2O_3	250–800	1.828	2.496	–0.106	1.889	TE
Dy_2O_3	250–800	1.876	2.219	0.082	1.932	TE
Ho_2O_3	250–800	1.902	1.848	–0.056	1.947	TE
Er_2O_3	250–800	1.903	1.018	0.345	1.931	TE
Yb_2O_3	250–800	2.002	1.727	0.004	2.045	TE
Lu_2O_3	250–800	1.807	1.476	0.034	1.844	TE
Oxides of elements of group II						
MgO	250–1100	1.666	1.254	–0.191	1.696	OM CVD
Oxides of elements of group III						
Al_2O_3	250–1100	1.608	0.196	0.097	1.614	OM CVD
Oxides and nitrides of elements of group IV						
SiO_2	250–1100	1.447	0.374	–0.003	1.457	Palik [20]
GeO_2	340–1100	1.555	0.865	0.251	1.578	Nunley [21]
Si_3N_4	400–1100	1.936	4.204	–2.649	2.024	CVD
TiO_2	500–900	2.252	2.924	4.047	2.350	OM CVD
ZrO_2	250–1100	2.097	1.005	1.275	2.130	IBSD
HfO_2	250–100	1.955	1.481	0.515	1.995	IBSD
Oxides of elements of group V						
V_2O_5	500–900	2.450	–6.550	55.400	2.632	IBSD
Ta_2O_5	350–1100	2.050	1.871	2.641	2.089	IBSD
Mixed oxides						
$Hf_xZr_{1-x}O_2$	250–1100	2.087	–0.711	2.029	2.082	IBSD

The objective of this work is to study the dispersion of the refractive index in dielectrics with a high dielectric permittivity, high-*k* dielectrics.

EXPERIMENTAL TECHNIQUE

All oxide films examined in this work (see Table 1), which are considered in microelectronics as high-*k* dielectrics, were obtained by thermal evaporation (TE), reactive ion-beam-sputtering deposition (IBSD), and chemical-vapor deposition using organometallic precursors (OM CVD). Oxide films were deposited on preliminarily prepared silicon substrates. The thickness of all oxide films was in the range of 40–100 nm. Their synthesis, surface morphology, and physicochemical properties were described previously in [15–19]. Silicon dioxide (glass) from the Palik database [20] and germanium dioxide are exceptions; the data from [21] are presented in Table 1 for comparison. For more convenient surveying, the oxides listed in the table are grouped over groups of the Mendeleev periodic table of elements.

Films of rare-earth oxides were obtained by thermal evaporation of corresponding metals in a vacuum of $(2–5) \times 10^{-5}$ Torr and subsequent oxidation of the metal film in a quartz furnace in air at 550°C for 30 min. As substrates, we used silicon *p*-Si(100) wafers with a resistance of $\rho \approx 5–10\ \Omega \times$ cm. For the properties of the surface of a silicon wafer to be reproducible, a layer of thermal SiO_2 with a thickness of ~100 nm was preliminarily grown on the wafer in dry oxygen at a temperature of 950°C. Prior to the metal deposition, the obtained thermal SiO_2 was etched in an aqueous solution of HF (48%), after which the silicon wafer

was washed in deionized water. The thickness of oxide films of rare-earth elements ranged from 30 to 90 nm. The procedure for the preparation of oxides of rare-earth elements has been described greater detail in [15, 16].

Measurements of samples were performed using an Ellips-1881 spectral ellipsometer; the wavelength range was 250–800 nm, and the angle of incidence of light was $\varphi = 70°$ [22]. The four-zone measurement technique was used, the measurement accuracy of ellipsometric angles ψ and Δ was not worse than 0.1° and 0.2°, respectively. This made it possible to obtain precise data on the optical properties of the films under study and to calculate the spectral dependences of their refractive index $n(\lambda)$.

All the films examined in this work were transparent in the used spectral range. Therefore, obtained dependences $n(\lambda)$ were described using the Cauchy dispersion formula

$$n(\lambda) = n_0 + \frac{A}{\lambda^2} + \frac{B}{\lambda^4}, \quad (1)$$

where n_0, A, and B are constants, which were selected for each sample with the Levenberg–Marquardt algorithm so as to minimize discrepancies between measured and calculated spectra of ellipsometric parameters. As a numerical comparison test for the spectra, we used the objective function

$$\chi = \frac{1}{2n - m - 1}\sum_{i=1}^{n}(|\Psi_e^i - \Psi_c^i| + |\Delta_e^i - \Delta_c^i|). \quad (2)$$

Here, Ψ_e^i, Δ_e^i, and Ψ_c^i, Δ_c^i are the measured (e) and calculated (c) values of the ellipsometric parameters at the ith wavelength; n is the number of wavelengths at which the fitting was performed; and m is the number of sought parameters. The calculated values of the ellipsometric parameters were obtained in accordance with a single-layer model of the optical system using a homogeneous layer with sharp boundaries [23].

At the first step, three parameters, n_0, A, and film thickness d at a zero value of coefficient B, were determined. If the involvement of parameter B in the search did not lead to a decrease in the objective function or reduced it by less than 10%, then the dispersion dependence of $n(\lambda)$ was described by the first two terms in (1); otherwise, term $\frac{B}{\lambda^4}$ was added. For the majority of samples, the involvement of the optical absorption in the layer under investigation also slightly improved the coincidence between the spectra and reduced the value of the objective function. However, the question of whether there is a weak absorption in the films (absorption index k is either smaller than 0.01 or is on the order of this value) or it is possible to compensate in this way for some discrepancies between the real structure and the used optical model, remains open. Attempts were also made to complicate the model by including into it a transition layer between the boundary of the film and the substrate, as well as a surface layer, which takes into account the contribution of the surface microroughness to measurement results. Upon including these layers into the model, we observed that the objective function either remained unchanged, or insignificantly decreased (within 10%). It can be concluded from this that the films studied in this work are homogeneous over thickness and composition and that a single-layer model with sharp boundaries serves as a good approximation for the interpretation of measured spectra.

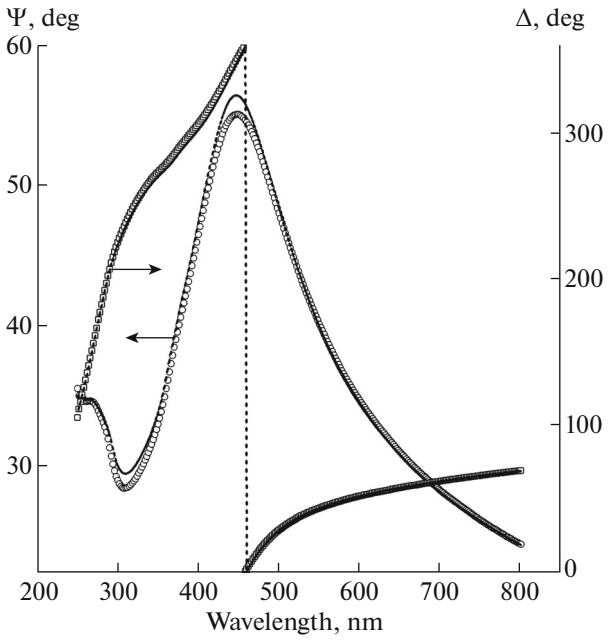

Fig. 1. Experimental (symbols) and calculated (curves) of dependences $\Psi(\lambda)$ and $\Delta(\lambda)$ for an Er_2O_3 film on silicon. The film thickness is 66.4 nm.

RESULTS AND DISCUSSION

Figure 1 shows the measured and calculated spectra for an Er_2O_3 film. The shapes of spectral dependences $\Psi(\lambda)$ and $\Delta(\lambda)$ are characteristic of thin transparent dielectric films [24]. A good coincidence between the presented calculated spectra $\Psi(\lambda)$ and $\Delta(\lambda)$ and the experimental spectra means that the used single-layer optical model adequately describes the structure of the sample.

Figures 2 and 3 show the spectral dependences of the refractive indices for oxides of rare-earth and other metals, and Table 1 presents the corresponding values of parameters n_0, A, and B of the dispersion relations calculated in the indicated spectral ranges in accordance with dispersion model (1). The values of the refractive indices at the wavelength of 632.8 nm of a He–Ne laser (which is most frequently used in ellip-

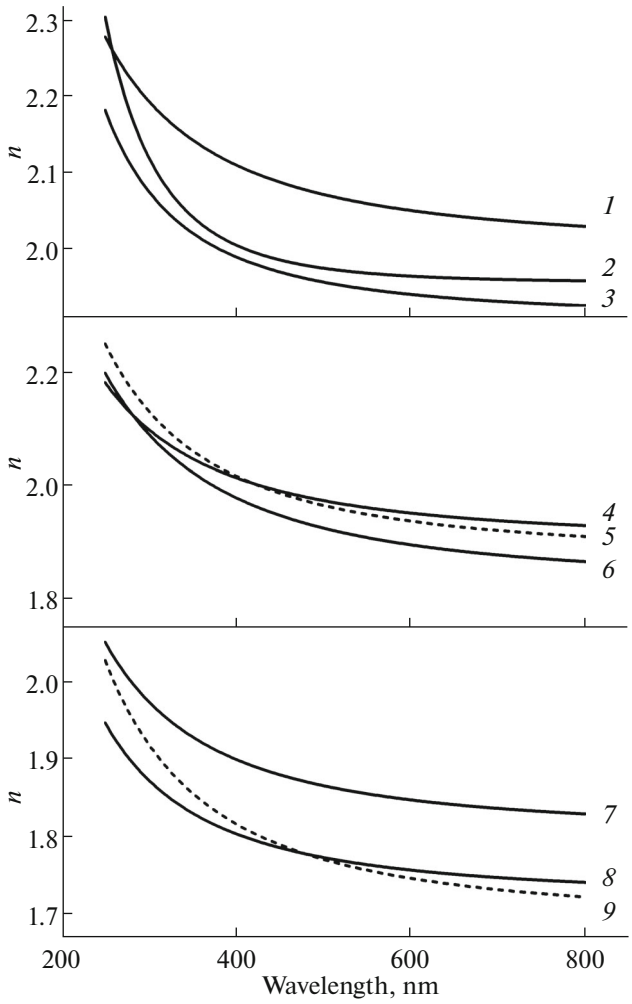

Fig. 2. Dispersion dependences $n(\lambda)$ calculated by Cauchy model (3) for films of oxides of rare-earth metals: (*1*) Yb_2O_3, (*2*) Sc_2O_3, (*3*) Er_2O_3, (*4*) Ho_2O_3, (*5*) Dy_2O_3, (*6*) Gd_2O_3, (*7*) Lu_2O_3, (*8*) La_2O_3, and (*9*) Y_2O_3.

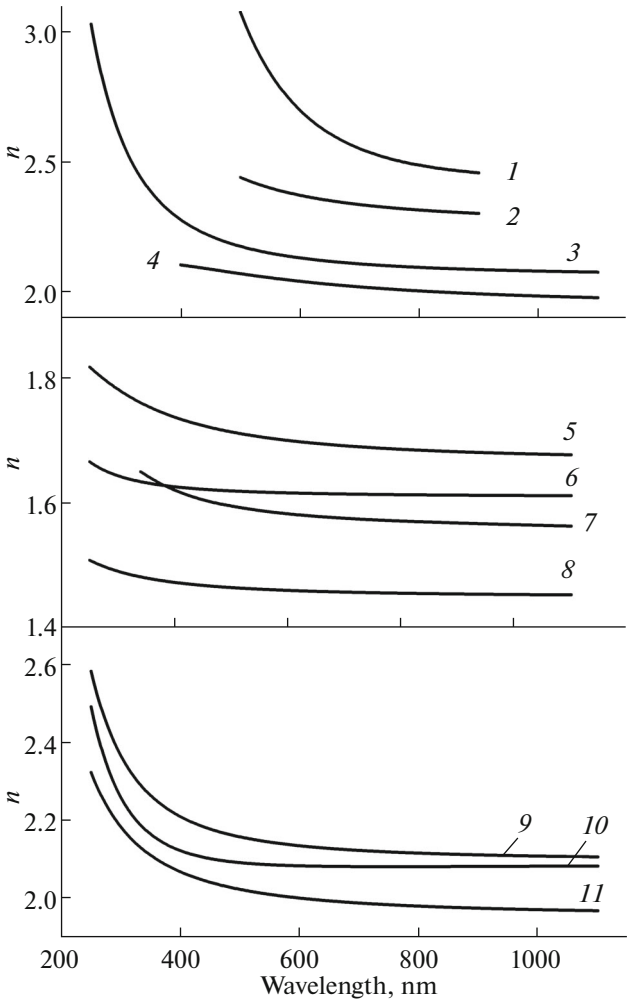

Fig. 3. Dispersion dependences $n(\lambda)$ calculated by Cauchy model (3) for films of oxides of metals from groups II–V: (*1*) V_2O_5, (*2*) TiO_2, (*3*) Ta_2O_5, (*4*) Si_3N_4, (*5*) MgO, (*6*) Al_2O_3, (*7*) GeO_2, (*8*) SiO_2, (*9*) ZrO_2, (*10*) $Hf_xZr_{1-x}O_2$, and (*11*) HfO_2.

someters for technological monitoring) are also listed in Table 1.

It is seen from Fig. 2 and Table 1 that the dispersion dependences of rare-earth metal oxides have a wide range of $n(\lambda)$: the values of the refractive index, measured at $\lambda = 632.8$ nm, vary in the range between 1.741 (for Y_2O_3) and 2.045 (for Yb_2O_3). The wide range of $n(\lambda)$ and similar structural and physicochemical properties of rare-earth oxides make it possible to obtain films of mixed rare-earth oxides of high quality with predetermined optical properties, calculated in accordance with the theory of effective medium [25]. For convenience, the dependences $n(\lambda)$ are presented in Fig. 2 in three groups. The upper part of the figure refers to oxides with high values of the dispersion (Yb_2O_3, Sc_2O_3, and Er_2O_3); in the middle, the dependences for oxides with intermediate values of the dispersion are presented (Ho_2O_3, Dy_2O_3, and Gd_2O_3); and the lower part of the figure shows the dependences for oxides with low values of the dispersion (Lu_2O_3, La_2O_3, and Y_2O_3).

The dispersion dependences of the remaining oxides are shown in Fig. 3, and they also were divided into three groups. The data for oxides and silicon nitride (V_2O_5, TiO_2, Ta_2O_5, and Si_3N_4) with a high dispersion (the values of n at $\lambda = 632.8$ nm exceed 2) are presented in the upper part of the figure). The dependences for oxides with a low dispersion (Mg, Al, Si, and Ge oxides) are shown in the middle part of the figure. And the lower part of the figure refers to HfO_2 and ZrO_2, which are oxides that are most widely used at present as high-k dielectrics; the dispersion dependence of a film of a mixed oxide, $Hf_xZr_{1-x}O_2$, is also shown here. Dispersion dependence $n(\lambda)$ for $Hf_xZr_{1-x}O_2$ (curve *10*) lies between dependences $n(\lambda)$ for ZrO_2

(curve *9*) and HfO_2 (curve *11*). Evaluations based on the Brüggemann model of an effective medium [25] allowed us to estimate quantity x to be ~0.65.

CONCLUSIONS

In this work, we briefly reviewed the optical properties of oxide materials that are employed at present in microelectronics as dielectrics. The results of the study can be used for further studies of the properties of dielectrics and in technologies for the design of new semiconductor instruments.

ACKNOWLEDGMENTS

This work was supported by the Russian Science Foundation, grants nos. 16-19-00002 (research involving HfO_2, ZrO_2, and Ta_2O_5) and 14-19-00192 (research involving $Hf_{0.5}Zr_{0.5}O_2$).

REFERENCES

1. V. A. Gritsenko, I. E. Tyschenko, V. P. Popov, and T. V. Perevalov, *Insulators in Nanoelectronics* (Sib. Otdel. RAN, Novosibirsk, 2010) [in Russian].
2. J. Robertson and R. M. Wallace, Mater. Sci. Eng. R **88**, 1 (2015).
3. T. V. Perevalov and V. A. Gritsenko, Phys. Usp. **53**, 561 (2010).
4. Y. Wang, Y.-T. Chen, F. Xue, F. Zhou, Y.-F. Chang, B. Fowler, and J. C. Lee, Appl. Phys. Lett. **100**, 083502 (2012).
5. A. S. Shaposhnikov, T. V. Perevalov, V. A. Gritsenko, C. H. Cheng, and A. Chin, Appl. Phys. Lett. **100**, 243506 (2012).
6. S. Kim, S. Jung, M.-H. Kim, S. Cho, and B.-G. Park, Appl. Phys. Lett. **106**, 212106 (2015).
7. D. R. Islamov, V. A. Gritsenko, C. H. Cheng, and A. Chin, Appl. Phys. Lett. **105**, 262903 (2014).
8. D. R. Islamov, V. A. Gritsenko, C. H. Cheng, and A. Chin, Optoelectron., Instrum. Data Process. **50**, 310 (2014).
9. S. Kumar, C. E. Graves, J. P. Strachan, E. M. Grafals, A. L. D. Kilcoyne, T. Tyliszczak, J. N. Weker, Y. Nishi, and R. S. Williams, Adv. Mater. **28**, 2772 (2016).
10. J. J. Yang, D. B. Strukov, and D. R. Stew, Nat. Nanotechnol. **8**, 13 (2013).
11. D. R. Islamov, A. G. Chernikova, M. G. Kozodaev, A. M. Markeev, T. V. Perevalov, V. A. Gritsenko, and O. M. Orlov, JETP Lett. **102**, 544 (2015).
12. K. A. Nasyrov and V. A. Gritsenko, Phys. Usp. **56**, 999 (2013).
13. J. Frenkel, Phys. Rev. **54**, 647 (1938).
14. D. S. Jeong, H. B. Park, and C. S. Hwang, Appl. Phys. Lett. **86**, 072903 (2005).
15. V. V. Kaichev, T. I. Asanova, S. B. Erenburg, T. V. Perevalov, V. A. Shvets, and V. A. Gritsenko, J. Exp. Theor. Phys. **116**, 323 (2013).
16. T. V. Perevalov, A. E. Dolbak, V. A. Shvets, V. A. Gritsenko, T. I. Asanova, and S. B. Erenburg, Eur. Phys. J. Appl. Phys. **65**, 10702 (2014).
17. V. N. Kruchinin, V. Sh. Aliev, A. K. Gerasimova, and V. A. Gritsenko, Opt. Spectrosc. **121**, 241 (2016).
18. V. V. Atuchin, V. A. Kochubey, L. D. Pokrovsky, V. N. Kruchinin, and C. V. Ramana, Opt. Spektosk. **117**, 438 (2014).
19. Yu. V. Shevtsov, B. M. Kuchumov, V. N. Kruchinin, E. V. Spesivtsev, I. F. Golovnev, and I. K. Igumenov, Phys. Proc. **46**, 27 (2013).
20. E. D. Palik, *Handbook of Optical Constants of Solids* (Academic, San Diego, 1985).
21. T. N. Nunley, N. S. Fernando, N. Samarasingha, J. M. Moya, C. M. Nelson, A. A. Medina, and S. Zollner, J. Vac. Sci. Technol. B **34**, 061205 (2016).
22. S. V. Rykhlitskii, E. V. Spesivtsev, V. A. Shvets, and V. Yu. Prokop'ev, Prib. Tekh. Eksp., No. 2, 161 (2012).
23. R. M. A. Azzam and N. M. Bashara, *Ellipsometry and Polarized Light* (North-Holland, Amsterdam, 1977).
24. C. V. Ramana, S. Utsunomiya, R. C. Ewing, U. Becker, V. V. Atuchin, V. Sh. Aliev, and V. N. Kruchinin, Appl. Phys. Lett. **92**, 011917 (2008).
25. S. Bosch, J. Ferre-Borrull, N. Leinfellner, and A. Canillas, Surf. Sci. **453**, 9 (2000).

Translated by V. Rogovoi